A Constrained Optimization Solution for Caughey Damping Coefficients in Seismic Analysis

Journal:	*Engineering Computations*
Manuscript ID	EC-12-2015-0404.R1
Manuscript Type:	Research Article
Keywords:	Caughey damping, seismic response analysis, modal damping ratios, constrained quadratic programming

A Constrained Optimization Solution for Caughey Damping Coefficients in Seismic Analysis

Danguang Pan [a,b] and Chenfeng Li [c, d *]

[a] *Department of Civil Engineering, University of Science and Technology Beijing, Beijing, 100083, China*
[b] *State Key Laboratory for Disaster Reduction in Civil Engineering, Tongji University, Shanghai, 200092, China*
[c] *Zienkiewicz Centre for Computational Engineering, Swansea University, Swansea SA2 7LZ, UK*
[d] *Energy Safety Research Institute, Swansea University, Swansea SA2 7LZ, UK*

Abstract: Extended from the classic Rayleigh damping model in structural dynamics, the Caughey damping model allows the damping ratios to be specified in multiple modes while satisfying the orthogonality conditions. Despite of these desirable properties, Caughey damping suffers from a few major drawbacks: (1) depending on the frequency distribution of the significant modes, it can be difficult to choose the reference frequencies that ensure reasonable values for all damping ratios corresponding to the significant modes; (2) it cannot ensure all damping ratios are positive. This paper presents a constrained quadratic programming approach to address these issues. The new method minimizes the error of the structural displacement peak based on the response spectrum theory, while all modal damping ratios are constrained to be greater than zero. The proposed method is highly efficient and allows the damping ratios to be conveniently specified for all significant modes, producing optimal damping coefficients in practical applications. Several comprehensive examples are presented to demonstrate the accuracy and effectiveness of the proposed method, and comparisons with existing approaches are provided whenever possible.

Key words: Caughey damping; seismic response analysis; modal damping ratios; constrained quadratic programming

1. Introduction

Properly specifying the damping matrix is critical in seismic analysis [1]. As many unquantifiable factors can cause damping, it is hard, if not impossible, to directly calculate the damping matrix from the dimensions and material parameters of structural members. In engineering practice, the damping matrix is constructed using measured or recommended damping values [2-5]. Owing to simplicity in mathematical treatment, the Rayleigh damping model is widely used in real-world problems such as frames [6], bridges [7, 8], dams [9] and domes [10]. Some non-classical damping matrices have also been proposed, e.g. for structures made up of more than one single type of materials [11] and for passively controlled structures [12] with supplemental damping facilities. Mánica etc. [13] showed that the Rayleigh damping turned out to be the most suitable alternative to represent energy dissipation of soil elements. Hall [14] investigated the effects of mass-proportional damping and stiffness-proportional damping, and suggested using the stiffness-proportional damping for nonlinear time-history seismic analysis. Ryan and Polanco [15] also recommended stiffness-proportional damping for the superstructure of base-isolated buildings. Hall [14], Zareian and Medina [16] and Jehel etc. [17] researched the updated tangent stiffness to calculate the Rayleigh coefficients for the effects of inelastic response. Base on shake table testing, Pant etc. [18] showed that the Rayleigh damping coefficients calculated with post-elastic stiffness

* **Corresponding author.**
E-mail addresses: pdg@ustb.edu.cn (D. G. Pan), c.f.li@swansea.ac.uk (C. F. Li)

results in relatively lower errors in peak response; updating damping coefficients in each step is time-consuming but does not substantially improve results. Whatever initial or tangent stiffness, it should specify two reference frequencies to calculate the Rayleigh coefficients.

It is well known that Rayleigh damping brings error to modal damping ratios with the exception of the two reference frequencies. Chopra [2] illustrated that the two reference modes should be carefully chosen to ensure reasonable damping ratios for all modes contributing significantly to the structural response. Tsai etc. [19] proposed that both the site frequency and the frequency characteristics should be considered to specify the two reference frequencies for the seismic response of soil layer. Taking the mode kinetic energy as the weight parameter, Yang etc. [20] developed a weighted least squares method to calculate Rayleigh damping coefficients. More recently, Pan etc. [21] proposed an optimization solution for Rayleigh damping coefficients, which greatly simplifies the determination of the two Rayleigh coefficients and eliminates the arbitrariness in the current experience-based practice.

Rayleigh damping works well when the modes contributing significantly to the structural response are distributed over a narrow frequency band. However, for many structures, the significant modes for different responses are different and the associated frequencies can differ significantly. For example, the top displacement of a building structure is dominated by the first several lower-frequency modes, while the responses corresponding to higher modes can be significant for the foundation force of cantilever structures [22]. In this case, Rayleigh damping cannot simultaneously ensure good accuracy for both displacements and forces. Hence, it is desirable to construct the damping matrix such that multiple modal damping ratios can be specified using the recommended/measured values.

Clough [3] proposed a damping matrix which sets lower order modal damping ratios equal to the recommended values by combining stiffness-proportional damping with superposition of modal damping. Dong [23] combined the Rayleigh damping and the superposition of modal damping. However, these approaches result in full damping matrices, thereby increasing computing time for a large-scale finite element model. In principle, the Caughey damping model [24] can also set multiple modal damping ratios equal to the exact value. Moreover, for lumped mass matrix systems, the band width of the resulting damping matrix will only increase proportionally when the length of the Caughey series grows. The Caughey damping matrix $\boldsymbol{c}$ is expressed as

$$\boldsymbol{c} = \boldsymbol{m}\sum_{l=0}^{J-1} a_l \left[\boldsymbol{m}^{-1}\boldsymbol{k}\right]^l \tag{1}$$

where $\boldsymbol{m}$ denotes the mass matrix, $\boldsymbol{k}$ the stiffness matrix, and a_l the Caughey damping coefficients. The unknown coefficients a_l can be evaluated by specifying J damping ratios ζ_l^* with reference frequencies ω_{rl} $\left(l = 1, 2, \cdots, J\right)$. That is

$$\boldsymbol{a} = \boldsymbol{\Omega}_r^{-T}\boldsymbol{y} \tag{2}$$

where $\boldsymbol{a} = \left\{a_0 \quad a_1 \quad \cdots \quad a_{J-1}\right\}^T$, $\boldsymbol{y} = \left\{\zeta_1^*, \zeta_2^*, \cdots, \zeta_J^*\right\}^T$, and $\boldsymbol{\Omega}_r = [\boldsymbol{\Omega}_{r1}, \boldsymbol{\Omega}_{r2}, \cdots, \boldsymbol{\Omega}_{rJ}]$ with $\boldsymbol{\Omega}_{ri} = \frac{1}{2}\left\{\omega_{ri}^{-1} \quad \omega_{ri} \quad \cdots \quad \omega_{ri}^{2J-1}\right\}^T$ $\left(i = 1, 2, \cdots, J\right)$. However, the following problems have hindered the wider application of Caughey damping: (1) Eq. (2) is ill-conditioned when the entries of Caughey damping matrix are of great magnitude; (2) no effective guidelines are presently available for choosing the reference frequencies that ensure reasonable modal damping ratios for all significant contribution modes; (3) negative damping coefficients can occur as a result of arbitrarily specifying the reference modes even when an even number of terms are included in Eq.

(1). For the first challenge outlined above, Luco [25] proposed a factorization method to obtain the solution for the ill-conditioned matrix. For the choice of reference frequencies, Clough [3] used equally spaced points between ω_{r1} and ω_{rJ}, and also suggested using an even number of terms in Caughey series. Here, ω_{r1} is the fundamental frequency and ω_{rJ} is the highest frequency of the significant modes. Choosing equally spaced points ignores the distinction of modal contribution, and as a result the calculation error cannot be controlled. Moreover, using an even number of terms in Caughey series does not avoid negative damping coefficients, especially for those frequencies near the endpoints.

To address the above deficiency associated with Caughey damping, an optimization approach is proposed here to determine Caughey damping coefficients and ensure all damping ratios of significant modes to take reasonable values. Specifically, based on the response spectrum theory, an objective function is formulated to minimize the peak displacement error of a structure. By enforcing all modal damping ratios to be positive, a constrained quadratic programming scheme is formulated to calculate the Caughey damping coefficients. The proposed method has the following advantages: (1) there is no need to specify the reference frequencies, and instead the method directly obtains Caughey damping coefficients that ensures reasonable modal damping ratios for all significant modes; (2) all modal damping ratios are positive. The new method makes the Caughey damping model both accurate and computationally efficient, and thus suitable for time history analysis of large complex structures.

2. Formulation for optimal Caughey damping coefficients

For a multi-degree of freedom (MDOF) structure under seismic acceleration excitation, the equation of motion for the forced vibration can be expressed as

$$\boldsymbol{m}\ddot{\boldsymbol{u}}+\boldsymbol{c}\dot{\boldsymbol{u}}+\boldsymbol{k}\boldsymbol{u}=-\boldsymbol{m}\boldsymbol{I}\ddot{u}_g(t) \tag{3}$$

where $\boldsymbol{u}$, $\dot{\boldsymbol{u}}$ and $\ddot{\boldsymbol{u}}$ are the relative displacement, velocity and acceleration vectors, respectively, $\boldsymbol{I}$ is the ground motion influence vector, $\ddot{u}_g(t)$ is the acceleration of ground motion, and $\boldsymbol{c}$ is the damping matrix as defined in Eq. (1). Given the first N-order natural frequencies ω_n (n = 1, 2, …, N) and the associated mode shapes $\boldsymbol{\phi}_n$, the approximate displacement of the structure can be expressed as a linear combination of N modal coordinates $q_n(t)$:

$$\boldsymbol{u}(t)\approx\sum_{n=1}^{N}\boldsymbol{\phi}_n q_n(t)\,. \tag{4}$$

Then, the uncoupled equation for the n^{th} mode of vibration is

$$\ddot{q}_n(t)+2\zeta_n\omega_n\dot{q}_n(t)+\omega_n^2 q_n(t)=-\gamma_n\ddot{u}_g(t) \tag{5}$$

where $\gamma_n=-\boldsymbol{\phi}_n^T\boldsymbol{m}\boldsymbol{I}/M_n$ is the modal participation factor, and $M_n=\boldsymbol{\phi}_n^T\boldsymbol{m}\boldsymbol{\phi}_n$ is the modal mass. The approximate modal damping ratio ζ_n can be expressed as:

$$\zeta_n=\boldsymbol{\Omega}_n^T\boldsymbol{a} \tag{6}$$

where $\boldsymbol{\Omega}_n=\frac{1}{2}\left\{\omega_n^{-1}\quad\omega_n\quad\cdots\quad\omega_n^{2J-1}\right\}^T$. Let u_{kn} denote the approximate peak displacement responses contributed by the n^{th} mode of vibration to the k^{th} degree of freedom of the structure, and u_{kn}^* the exact peak displacement response. Following the definition of the deformation response spectrum [2, 21], u_{kn} and u_{kn}^* can be expressed as

$$u_{kn}=\gamma_n\phi_{kn}S_d(\zeta_n,\omega_n) \tag{7}$$

$$u_{kn}^{*} = \gamma_n \phi_{kn} S_d(\zeta_n^{*}, \omega_n) \tag{8}$$

where $S_d(\zeta, \omega_n) = \left| \frac{1}{\omega_{nD}} \int_0^t \ddot{u}_g(\tau) e^{-\zeta\omega_n(t-\tau)} \sin\left[\omega_{nD}(t-\tau)\right] d\tau \right|_{\max}$ is the deformation response spectrum with $\omega_{nD} = \omega_n \sqrt{1-\zeta^2}$. The term ϕ_{kn} is the n^{th} mode value at the k^{th} degree of freedom. When the exact modal damping ratio ζ_n^{*} is used in the evaluation of spectral response, the peak response is u_{kn}^{*} correspondingly.

An objective function can be formulated to represent the total error E_k of the peak response at the k^{th} degree of freedom of the structure:

$$E_k = \sqrt{\sum_{n=1}^{N} \gamma_n^2 \phi_{kn}^2 [S_d(\zeta_n^{*}, \omega_n) - S_d(\zeta_n, \omega_n)]^2} \,. \tag{9}$$

The objective function E_k is an implicit function of the damping coefficient $\boldsymbol{a}$ through $S_d(\zeta_n, \omega_n)$ and ζ_n. To simplify this highly nonlinear relation, the deformation response spectrum $S_d(\zeta_n, \omega_n)$ is expanded into the first-order Taylor series:

$$S_d(\zeta_n, \omega_n) \approx S_d(\zeta_n^{*}, \omega_n) + S_d'(\zeta_n^{*}, \omega_n)(\zeta_n - \zeta_n^{*}) \tag{10}$$

where $S_d'(\zeta_n^{*}, \omega_n) = \partial S_d(\zeta_n^{*}, \omega_n) / \partial \zeta_n$. Substituting Eq. (10) into Eq. (9) yields

$$E_k^2(\boldsymbol{a}) = \left(\boldsymbol{\Omega}^T \boldsymbol{a} - \boldsymbol{y}\right)^T \bar{\boldsymbol{w}} \left(\boldsymbol{\Omega}^T \boldsymbol{a} - \boldsymbol{y}\right) \tag{11}$$

where $\boldsymbol{y} = \left\{\zeta_1^{*}, \zeta_2^{*}, \cdots, \zeta_N^{*}\right\}^T$, $\bar{\boldsymbol{w}} = \text{diag}\left\{\bar{w}_{k1}, \bar{w}_{k2}, \cdots, \bar{w}_{kN}\right\}$, $\bar{w}_{kn} = \gamma_n^2 \phi_{kn}^2 S_d'^2$, and $\boldsymbol{\Omega} = [\boldsymbol{\Omega}_1, \boldsymbol{\Omega}_2, \cdots, \boldsymbol{\Omega}_N]$. To simplify the equation, the weight coefficients are normalized as:

$$w_{kn} = \bar{w}_{kn} / \sum_{i=1}^{N} \bar{w}_{ki} \,. \tag{12}$$

Under a given excitation, some of the weight coefficients will vanish, especially when mode shapes are orthogonal with the loading influence vector. Combining only those modes with weight coefficients exceeding a given threshold $w_{\min}$, the objective function can be rewritten as

$$f(\boldsymbol{a}) = \left(\boldsymbol{\Omega}^T \boldsymbol{a} - \boldsymbol{y}\right)^T \boldsymbol{w} \left(\boldsymbol{\Omega}^T \boldsymbol{a} - \boldsymbol{y}\right). \tag{13}$$

To minimize $f(\boldsymbol{a})$, the first derivatives of $f(\boldsymbol{a})$ with respect to $\boldsymbol{a}$ is set to zero, and the unconstrained optimal solution can be obtained as:

$$\boldsymbol{a} = \left[\boldsymbol{\Omega} \boldsymbol{w} \boldsymbol{\Omega}^T\right]^{-1} \boldsymbol{\Omega} \boldsymbol{w} \boldsymbol{y} \,. \tag{14}$$

For Caughey series with J terms, Eq. (14) is consistent with the conventional solution shown in Eq. (2) when all J reference modes are included in the computation. However, like the conventional solution, Eq. (14) cannot avoid negative damping ratios, which are unrealistic. Thus, it is necessary to enforce

$$\zeta_n = \boldsymbol{\Omega}_n^T \boldsymbol{a} > 0 \,. \tag{15}$$

In order to avoid the impractical amplification of undamped modal responses, a threshold $\zeta_{\min}$ representing the minimum modal damping ratio can be introduced for an optimal solution. Then, the constrained quadratic programming problem of $\boldsymbol{a}$ can be expressed as:

$$\text{minimize } f(\boldsymbol{a}) = \left(\boldsymbol{\Omega}^T \boldsymbol{a} - \boldsymbol{y}\right)^T \boldsymbol{w} \left(\boldsymbol{\Omega}^T \boldsymbol{a} - \boldsymbol{y}\right) \tag{16a}$$

$$\text{subject to: } \boldsymbol{\Omega}'^T \boldsymbol{a} \geq \boldsymbol{y}'_{\min} \tag{16b}$$

When the number of different natural frequency in Eq. (16) is no less than J, $\boldsymbol{\Omega} \boldsymbol{w} \boldsymbol{\Omega}^T$ is a positive definite matrix. The matrix $\boldsymbol{\Omega}'$ is a subset of $\boldsymbol{\Omega}$ consisting of all columns with different natural frequencies. Therefore, $\boldsymbol{\Omega}'$ has full column rank. All entries of $\boldsymbol{y}'_{\min}$ are set as

$\zeta_{\min}$. Eq. (16) defines a convex quadratic programming problem, for which the global optimal solution can be easily obtained [26]. In this paper, the active set method [26] is adopted to solve Eq. (16), for which the details are explained in the next section. It can be a time-consuming task in real-world engineering applications to search for J reference modes that locally minimize the total error E_k and ensure all modal damping ratios are positive. Therefore, unless otherwise noted, this study always includes all vibration modes of interest in Eq. (16) to solve the optimal Caughey damping coefficients.

3. The solution scheme

3.1 Formulation based on the active set method

Let $\boldsymbol{a}^{(k)}$ denote the feasible solution of Eq. (16) obtained in the k^{th} iteration, and the corresponding index set of the active constraints is:

$$I(\boldsymbol{a}^{(k)}) \subseteq \left\{ n \middle| -\boldsymbol{\Omega}_{cn}^T \boldsymbol{a} + \zeta_{\min} = 0, n \in J_s \right\} \tag{17}$$

where $J_s = \{1, 2, \cdots, N\}$ is the index set of the constraints in Eq. (16b), and $\boldsymbol{\Omega}_{cn} = \frac{1}{2}\left\{ \omega_{cn}^{-1} \quad \omega_{cn} \quad \cdots \quad \omega_{cn}^{2J-1} \right\}^T \quad n \in I(\boldsymbol{a}^{(k)})$. Then, we solve the following quadratic programming problem with equality constraints

$$\text{minimize } f(\boldsymbol{a}) = \left(\boldsymbol{\Omega}^T \boldsymbol{a} - \boldsymbol{y}\right)^T \boldsymbol{w} \left(\boldsymbol{\Omega}^T \boldsymbol{a} - \boldsymbol{y}\right) \tag{18a}$$

$$\text{subject to: } -\boldsymbol{\Omega}_{cn}^T \boldsymbol{a} + \zeta_{\min} = 0 \quad n \in I(\boldsymbol{a}^{(k)}) \tag{18b}$$

Eq. (18) can be solved via the standard Lagrange multiplier approach

$$\begin{bmatrix} \boldsymbol{G} & \boldsymbol{\Omega}_c \\ \boldsymbol{\Omega}_c^T & 0 \end{bmatrix} \begin{Bmatrix} \boldsymbol{a} \\ \boldsymbol{\lambda} \end{Bmatrix} = \begin{Bmatrix} \boldsymbol{r} \\ \boldsymbol{b} \end{Bmatrix} \tag{19}$$

where $\boldsymbol{G} = \boldsymbol{\Omega} \boldsymbol{w} \boldsymbol{\Omega}^T$, $\boldsymbol{r} = \boldsymbol{\Omega} \boldsymbol{w} \boldsymbol{y}$, $\boldsymbol{\Omega}_c = -[\boldsymbol{\Omega}_{c1}, \boldsymbol{\Omega}_{c2}, \cdots, \boldsymbol{\Omega}_{cm}]$ and $\boldsymbol{b} = -\{\zeta_{\min}\}$. Denoted by $\bar{\boldsymbol{a}}^{(k)}$ and $\boldsymbol{\lambda}^{(k)}$, the solution of Eq. (19) has two possibilities: either $\bar{\boldsymbol{a}}^{(k)} \neq \boldsymbol{a}^{(k)}$ or $\bar{\boldsymbol{a}}^{(k)} = \boldsymbol{a}^{(k)}$.

If $\bar{\boldsymbol{a}}^{(k)} = \boldsymbol{a}^{(k)}$, the iteration can continue in two directions depending on the minimum entry of $\boldsymbol{\lambda}^{(k)}$ expressed as

$$\lambda_q^{(k)} = \min \left\{ \lambda_n^{(k)} \middle| n \in I(\boldsymbol{a}^{(k)}) \right\}. \tag{20}$$

If $\lambda_q^{(k)} \geq 0$, it means that $\boldsymbol{a}^{(k)}$ is the unique global solution and the iteration can be terminated. Otherwise, $\boldsymbol{a}^{(k+1)}$ is updated with $\boldsymbol{a}^{(k)}$, and the active set $I(\boldsymbol{a}^{(k+1)})$ at $\boldsymbol{a}^{(k+1)}$ is formed by removing the index q from $I(\boldsymbol{a}^{(k)})$, after which the next iteration begins from solving Eq. (18) with the updated initial value $\boldsymbol{a}^{(k+1)}$ and active set $I(\boldsymbol{a}^{(k+1)})$.

If $\bar{\boldsymbol{a}}^{(k)} \neq \boldsymbol{a}^{(k)}$, the initial value for the next iteration is given by

$$\boldsymbol{a}^{(k+1)} = \boldsymbol{a}^{(k)} + \alpha_k \boldsymbol{d}^{(k)} \tag{21}$$

where $\boldsymbol{d}^{(k)} = \bar{\boldsymbol{a}}^{(k)} - \boldsymbol{a}^{(k)}$, and α_k is determined as

$$\alpha_k = \min\{1, \alpha_p\}, \quad \alpha_p = \min_{\substack{\boldsymbol{\Omega}_n^T \boldsymbol{d}^{(k)} < 0, \\ n \notin I(\boldsymbol{a}^{(k)})}} \frac{\boldsymbol{\Omega}_n^T \boldsymbol{a}^{(k)} - \zeta_{\min}}{-\boldsymbol{\Omega}_n^T \boldsymbol{d}^{(k)}}. \tag{22}$$

If $\alpha_k < 1$, the active set $I(\boldsymbol{a}^{(k+1)})$ at $\boldsymbol{a}^{(k+1)}$ is formed by adding the index p into $I(\boldsymbol{a}^{(k)})$, otherwise $I(\boldsymbol{a}^{(k+1)}) = I(\boldsymbol{a}^{(k)})$. Then, Eq. (18) is solved again with the updated $\boldsymbol{a}^{(k+1)}$ and $I(\boldsymbol{a}^{(k+1)})$.

The active set method requires an initial feasible solution $\boldsymbol{a}^{(0)}$ that satisfies Eq. (16). It is well known that the damping ratios of Rayleigh damping are always larger than zero, therefore, the initial feasible solution $\boldsymbol{a}^{(0)}$ can be set as

$$\boldsymbol{a}^{(0)} = \left\{ a_0^{(0)} \quad a_1^{(0)} \quad 0 \quad \cdots \quad 0 \right\}^T \tag{23}$$

$$\begin{Bmatrix} a_0^{(0)} \\ a_1^{(0)} \end{Bmatrix} = \frac{2\omega_1\omega_N}{\omega_N{}^2 - \omega_1{}^2} \begin{bmatrix} \omega_N & -\omega_1 \\ -\omega_N^{-1} & \omega_1^{-1} \end{bmatrix} \begin{Bmatrix} \zeta_1^* \\ \zeta_N^* \end{Bmatrix} \tag{24}$$

where ω_1 and ω_N are the fundamental frequency and the highest calculated frequency respectively. In this work, $\zeta_{\min}$ is set as

$$\zeta_{\min} = \min\left\{ \frac{\zeta^*}{10}, \min\left\{ \frac{a_0^{(0)}}{4\omega_n} + \frac{a_1^{(0)}\omega_n}{4}, (n = 1, 2, \cdots, N) \right\} \right\}. \tag{25}$$

Since $\boldsymbol{\Omega}'^T \boldsymbol{a}^{(0)} > \boldsymbol{y}'_{\min}$, the initial active set $I(\boldsymbol{a}^{(0)})$ is a void set.

3.2 The algorithm workflow

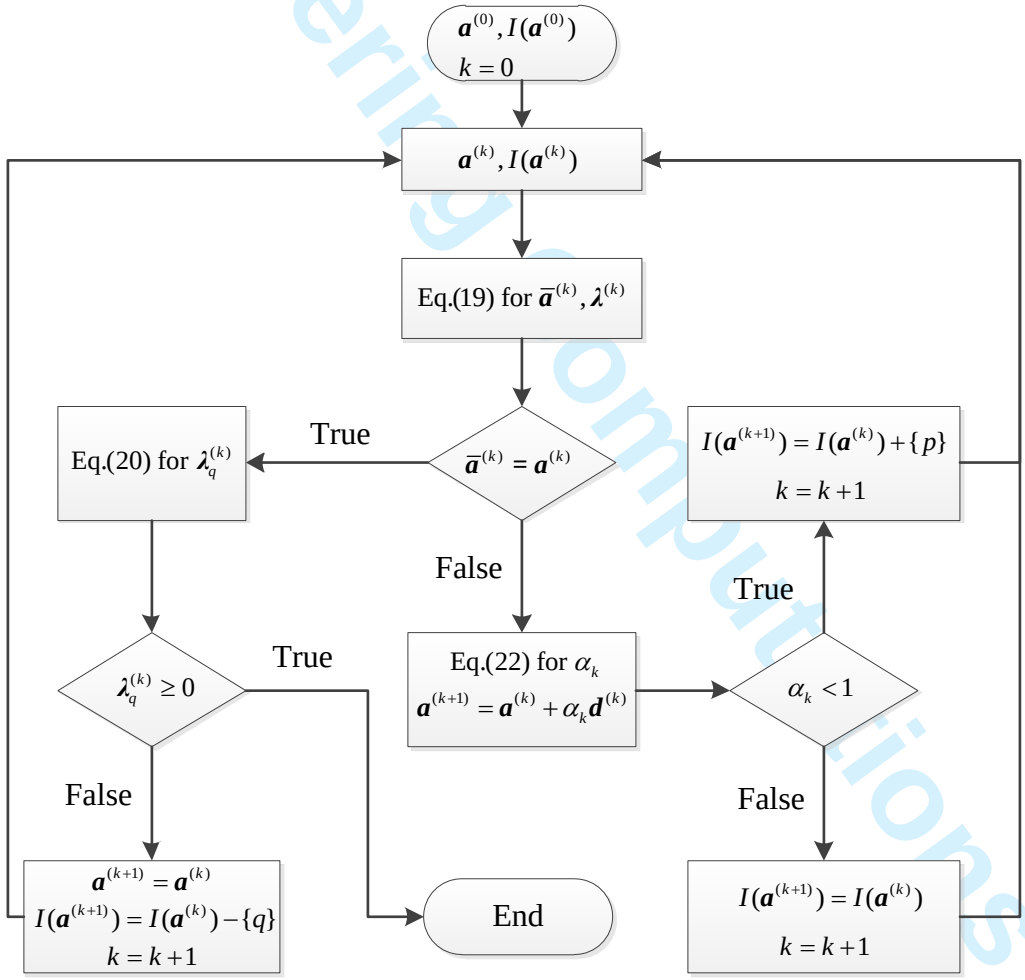

Figure 1 Flowchart of optimal solution

The workflow of the algorithm described above is shown in Figure 1, which is executed via four steps:

- Step 1: Set k=0, compute the initial feasible solution $\boldsymbol{a}^{(0)}$ from Eq. (23), and set the

active set $I(\boldsymbol{a}^{(0)})$ as a void set.

- Step 2: Compute $\bar{\boldsymbol{a}}^{(k)}$ and $\boldsymbol{\lambda}^{(k)}$ from Eq. (19). If $\bar{\boldsymbol{a}}^{(k)} = \boldsymbol{a}^{(k)}$, go to Step 3; otherwise go to Step 4.
- Step 3: Find $\lambda_q^{(k)}$ using Eq. (20). If $\lambda_q^{(k)} \geq 0$, output $\boldsymbol{a}^{(k)}$ as the solution and terminate the computation; otherwise, remove the index q from $I(\boldsymbol{a}^{(k)})$ to construct the active set $I(\boldsymbol{a}^{(k+1)})$, update $\boldsymbol{a}^{(k+1)}$ with $\boldsymbol{a}^{(k)}$, set k=k+1, and go back to Step 2.
- Step 4: Find α_k using Eq. (22) and set $\boldsymbol{a}^{(k+1)} = \boldsymbol{a}^{(k)} + \alpha_k \boldsymbol{d}^{(k)}$. If $\alpha_k < 1$, construct the active set $I(\boldsymbol{a}^{(k+1)})$ by adding the index p to $I(\boldsymbol{a}^{(k)})$; otherwise, let $I(\boldsymbol{a}^{(k+1)}) = I(\boldsymbol{a}^{(k)})$. Then set k=k+1 and go back to Step 2.

4. Parametric studies

4.1 Necessity of Caughey damping

To illustrate the necessity of Caughey damping, a dynamic analysis is conducted on a seven-story frame [22], which has many significant contribution modes with large differences in natural frequencies of the significant contribution modes for different responses. The idealized computer model is shown in Figure 2. The height of each story is 3m and the span between neighboring columns is 4m. The density and elastic modulus of the material are 7850kg/m^3 and 200GPa, respectively. The details of structural components are given in Table 1. Using the lumped-mass, the frame has 70 possible mode shapes. The significant contribution modes for lateral and vertical vibration are shown in Table 2. For the lateral vibration, the first three mode shapes are enough to approximate the lateral vibration due to the fact that their accumulated mass participation percentage is more than 90%. However, to obtain the 90% mass participation factors in the vertical direction, it will require 24 mode shapes. The exact damping ratio is 2% for all modes of vibration.

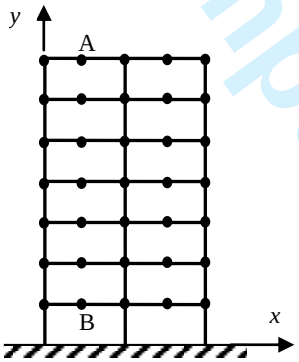

Figure 2 Model of a seven-story frame

Table 1 Details of structural components

Structural component	Story number	Cross-sectional area ($10^{-3}m^2$)	Area moment of inertia ($10^{-5}m^2$)	Added mass (10^3kg/m)
Beam	1-2	5.624	6.120	7.0
	3-4	3.976	2.740	4.2
	5-7	2.725	1.040	1.6
Side-column	1-2	11.60	16.28	0
	3-4	7.600	4.585	0
	5-7	6.144	3.781	0
Mid-column	1-2	24.00	36.16	0
	3-4	16.00	10.77	0
	5-7	16.00	10.77	0

Table 2 Results of modal analysis of the frame

Mode	Frequency (Hz)	Lateral mass participating factor		Vertical mass participating factor	
		Each (%)	Accumulated (%)	Each (%)	Accumulated (%)
1	0.537	55.379	55.379	0	0
2	1.206	22.369	77.748	0	0
3	2.252	12.847	90.596	0	0
9	6.166	0	95.687	38.121	38.121
11	6.473	0	95.687	2.253	40.735
18	7.420	0	99.665	7.715	48.874
20	7.670	0	99.930	14.640	63.514
24	17.785	0	99.999	25.530	90.018
32	36.897	0	99.999	2.809	92.840
34	39.306	0	99.999	4.304	97.144
70	157.676	0	100	0	100

Suppose that the building is subjected to vertical harmonic ground motion excitations:

$$\ddot{u}_g(t) = \sin\theta_1 t + \sin\theta_2 t + \sin\theta_3 t \tag{26}$$

in which θ_1=0.7ω_9, θ_2=1.25ω_9 and θ_3=2.8ω_9. The peak vertical displacements of point A u_{yA} and point B u_{yB} as well as vertical foundation force F_N derived by different numbers of mode are summarized in Table 3. It can be seen that the response errors can be very large when the significant modes are not included in the mode-superposition model (e.g. u_{yB} with mode numbers 11 and 18), and the response error is greatly reduced when all the modes contributing significantly to the particular response are included. It is apparent that the displacements of u_{yA} and u_{yB} derived by the first 24 modes are almost the exact, but F_N is underestimated by 1.598%. The equivalent static forces $\boldsymbol{F}_n^s$ associated with the n^{th} mode response can be expressed as $\boldsymbol{F}_n^s = \omega_n^2 \boldsymbol{m}\boldsymbol{\phi}_n q_n$, hence the contribution of higher modes are larger for foundation force than the displacements of point A and point B. The result indicates that the higher mode truncation affects the foundation force more than it does on the displacements.

Table 3 Cumulative modal contributions

Number of Modes	u_{yA}		u_{yB}		F_N	
	Total(mm)	Errors(%)	Total(mm)	Errors(%)	Total(10^2kN)	Errors(%)
11	3.500	13.932	0.297	97.422	3.493	84.050
18	2.879	6.283	0.495	95.703	5.687	74.032
20	2.882	6.185	11.45	0.521	12.83	41.416
24	3.073	0.033	11.51	0	21.55	1.598
32	3.073	0.033	11.51	0	21.65	1.142
34	3.072	0	11.51	0	21.80	0.457
70	3.072	0	11.51	0	21.90	0

When Rayleigh damping is used to construct the damping matrix, two combinations were considered for the "reference" modes of vibration: i=9 & j=20 and i=9 & j=24. The errors of u_{yA}, u_{yB} and F_N are presented in Table 4. Note that the errors of u_{yA} are always smaller than 1%, but u_{yB} is overestimated by 7.906% for i=9 & j=24 and F_N is underestimated by 6.164% for i=9 & j=20. A closer examination indicates that θ_2 is close to ω_{20} and θ_3 is close to ω_{24}. As shown in Table 3, for the u_{yB} value, the 20th mode response dominates the modal responses. Thus, shown in Table 4, the combination of i=9 & j=24 makes the 20th modal damping ratios smaller than exact values, which causes the over-amplified response. For the F_N, the 24th mode response is significant. The combination of i=9 & j=20 makes the 24th modal damping ratios larger than exact values, which causes the response smaller than the exact value. The significant contribution modes for different responses are different. When there are three or more significant contribution modes with large differences between the associated natural frequencies, Rayleigh damping will cause considerable errors in parts of dynamic responses whose frequencies of significant contribution modes stray far from the two "reference" frequencies. It is necessary to establish a damping matrix which makes more than two modal damping ratios equal to exact values.

Table 4 Relative errors (%) of Rayleigh damping under harmonic excitation

	u_{yA}		u_{yB}		F_N	
	Peaks(mm)	Errors(%)	Peaks(mm)	Errors(%)	Peaks(10^2kN)	Errors(%)
i=9 & j=20	3.042	0.977	11.50	0.087	20.55	**6.164**
i=9 & j=24	3.073	0.033	12.42	**7.906**	22.54	2.922

4.2 Influences of exponent combination of Caughey series

In Eq. (1), the integer exponent l can vary in the range $-\infty < l < \infty$, but in practice, two specific schemes are often preferred. One scheme is the direct extension of Rayleigh damping [2] with $l = 0,1,\cdots,J-1$ which is referred to as the extended Rayleigh exponent approach. The other scheme, referred to as the symmetric exponent approach, sets the l values as close to zero as possible [3], e.g. $l = -1,0,1,2$ if four terms of Caughey Series are required. Clough suggested using equally spaced points between ω_{r1} and ω_{rJ} as reference frequencies, where ω_{r1} and ω_{rJ} are the fundamental frequency and the frequency of the highest mode that contributes significantly to the response. Let ω_{rJ} be ω_{24} (the corresponding accumulated mass participation percentage is more than 90%), and set ω_{r2}, ω_{r3}, …, $\omega_{r(J-1)}$ equally spaced within the frequency range. The Caughey damping coefficients are obtained by Eq. (2). Substituting the result into Eq. (6), the resulting damping ratio-frequency relation is shown in Figure 3.

As shown in Figure 3(a), the even number of terms of the extended Rayleigh exponent approach makes damping ratios increase monotonically beyond the controlled range, which is reasonable, and is used later in the paper. But an important point to note is that negative damping occurs in J=8 for the extended Rayleigh exponent approach. In the viewpoint of numerical analysis, the Caughey series can be seen as a polynomial interpolation. Due to the Runge's phenomenon [27], i.e. higher interpolation curves are extremely steep at the endpoints, there still exists the risk of negative modal damping ratios even when an even number of terms are included in Eq. (1). It is necessary to ensure all damping ratios of natural frequencies larger than zero.

As shown in Figure 3(b), the symmetric exponents approach has a serious defect such that the damping decreases monotonically with frequencies increasing above ω_{24} for J=4 and J=8. Modes with frequencies greater than the controlled range would be negative damping. This is unacceptable because the negative damping can lead to unpractical responses.

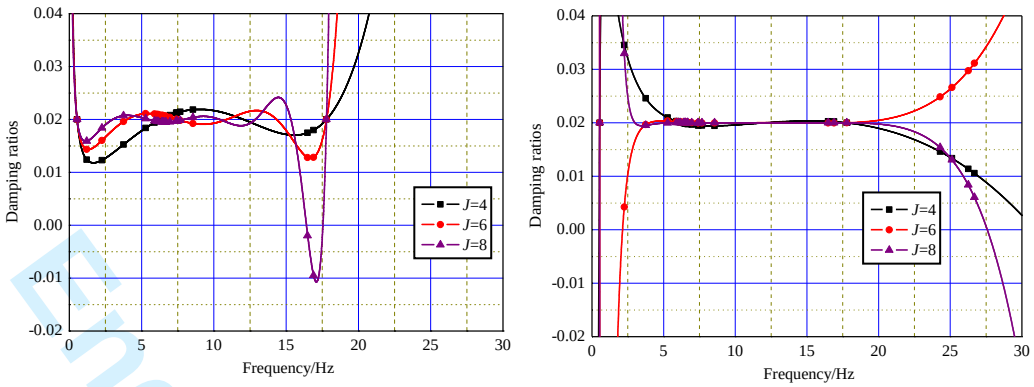

(a) The extended Rayleigh exponent approach (b) The symmetrical exponent approach

Figure 3 Damping ratio vs. frequency for various exponent combinations

4.3 Optimal modal damping ratios of Caughey damping

To investigate the characteristics of modal damping ratios obtained by Eq. (16) under the harmonic ground motion of Eq. (26) with $\theta_1 = 0.7\omega_9$, $\theta_2 = 1.25\omega_9$ and $\theta_3 = 2.8\omega_9$, the term number J is set to 2, 4, 6 and 8, respectively. In Eq. (16), an optimal DOF, termed the reference DOF, should be specified to construct the weighted matrix. In the discussion, the vertical displacements of point A and point B in Figure 2 are both selected as reference DOFs, to examine the impact of different reference DOFs on the optimization results. That is, $\phi_{kn} = \phi_n(\mathrm{A_y})$ or $\phi_n(\mathrm{B_y})$. For comprehensive optimal results, all significant modes should be included in Eq. (16) for optimization. To demonstrate the ability of finding the optimal reference frequencies using the proposed method, let N be 34. For comparison, two-, four-, six- and eight-term Caughey damping coefficients are determined by specified damping ratios, which is referred to as the conventional method in this paper. For this example, the reference frequencies are $\{\omega_9, \omega_{24}\}$ for J=2, $\{\omega_9, \omega_{18}, \omega_{20}, \omega_{24}\}$ for J=4, $\{\omega_9, \omega_{11}, \omega_{18}, \omega_{20}, \omega_{24}, \omega_{34}\}$ for J=6, $\{\omega_9, \omega_{11}, \omega_{15}, \omega_{18}, \omega_{20}, \omega_{24}, \omega_{32}, \omega_{34}\}$ for J=8. These reference frequencies are chosen according to their significant mass participating factors. At the same time, ω_{r1} and ω_{rJ} are set as ω_1 and ω_{34} for the endpoints of the equally spaced points, which is referred to as the equipartition method in this paper. The corresponding modal damping ratios are shown in Figure 4.

For the conventional method, negative damping occurs for J=6 and J=8, which indicates selecting arbitrary reference frequencies to construct the Caughey damping is inappropriate. It is possible to avoid negative damping ratios in the conventional method, but this requires tedious trial and error and the accuracy of dynamic responses cannot be estimated in advance. Therefore, the following parametric studies do not discuss the conventional method.

For the equipartition method, the negative modal damping appears again for J=8 due to Runge's phenomenon. Another defect of the equipartition method is that the effects of modal contributions are neglected. In this case, the specified frequencies would deflect from the significant contribution modes, and will cause uncontrollable errors of responses.

As for the optimization method, the damping curves also have negative values for J=8 due to the Runge phenomenon, but after applying the constraints all modal damping ratios are positive. Meanwhile, the optimization method makes the damping ratios of the significant contribution modes close to the exact values. Since the frequency content and significant modes of different DOFs are different, the choice of the reference DOF in ϕ_{kn} can affect the optimal damping coefficients. For example, the top displacement of $u_{y\mathrm{A}}$ is controlled by the first several modes, and the contribution from higher modes for $u_{y\mathrm{B}}$ are more significant than for $u_{y\mathrm{A}}$. Therefore the curves

of damping ratios based on $\phi_n(\mathrm{B}_y)$ move toward the side of higher frequency compared wtih $\phi_n(\mathrm{A}_y)$. Setting ϕ_{kn}=1 means that the peak of modal coordinates $q_n(t)$ is taken as the optimal objective due to $|q_n(t)|_{\max} = \gamma_n S_d(\zeta_n, \omega_n)$. It is equivalent to considering all degrees of freedom. Therefore, the higher frequencies effect is more significant and the curves appear to the right side among the three curves. Note that the modes used in optimal solution are all ortho-normalized relative to the mass matrix.

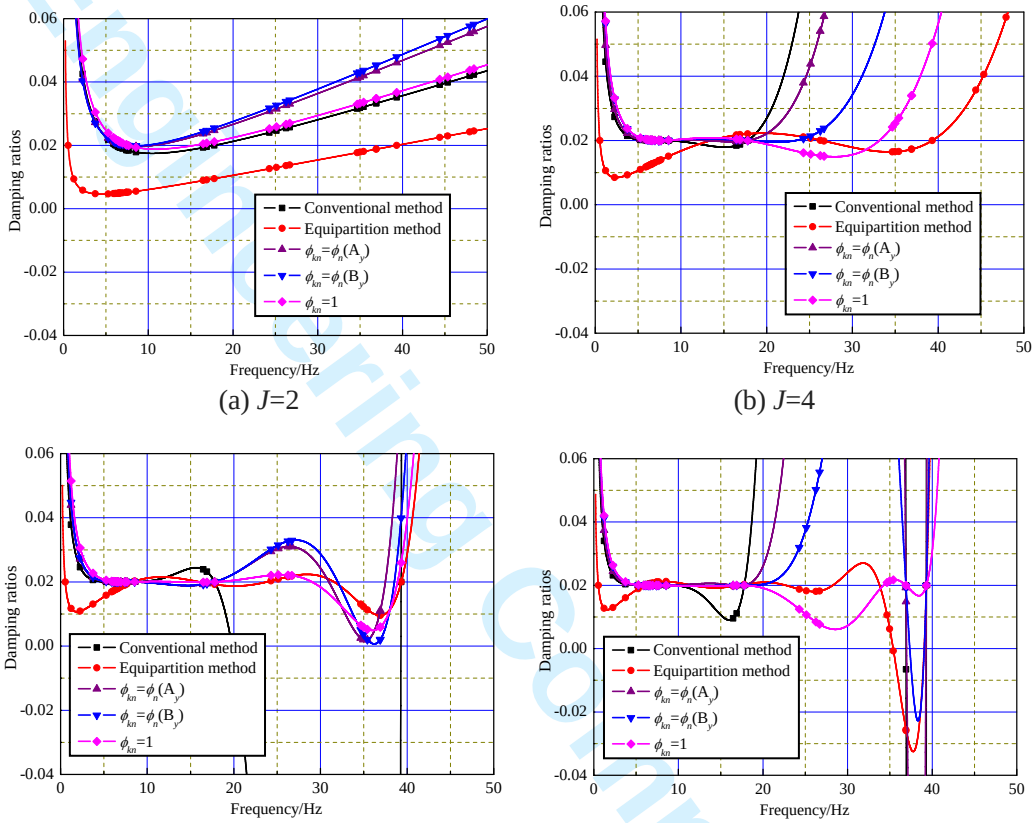

(a) J=2 (b) J=4

(c) J=6 (d) J=8

Figure 4 Damping ratio vs. frequency for various methods under harmonic excitations

4.4 The influences of mode numbers in optimal analysis

In Figure 4, the damping ratio curves for $J \geq 4$ are extremely steep at the endpoints and approaches to infinity rapidly as the frequency moves away from the interval [ω_{r1}, ω_{rJ}]. It implies that, equivalent to the truncation approach, the responses of modes with frequencies outside the range considered in evaluating the coefficients vanish even though all modes are included in the direct integration method. Therefore, the mode numbers which are used to optimal analysis in Eq. (16) should include all significant contribution modes. In order to analyze the source of errors, the relative error of response $e(N)$ based on Caughey damping is divided into truncation error $e_t(N)$ and convergence error $e_c(N)$.

$$e(N) = \frac{\left|r(N) - r^*\right|}{r^*} \times 100\% \tag{27a}$$

$$e_t(N) = \frac{\left|r_t(N) - r^*\right|}{r^*} \times 100\% \tag{27b}$$

$$e_c(N)=\frac{|r(N)-r_t(N)|}{r^*}\times 100\% \tag{27c}$$

in which r^* is the exact solution which can be obtained by mode superposition of all mode shapes with the exact damping ratios, $r_t(N)$ is the response which is evaluated by the first N modes with the exact damping ratios, and $r(N)$ is response when the highest reference frequency is associated with the Nth mode to construct Caughey damping. In the equipartition method, this indicates the right endpoint frequency ω_{rJ} is set as ω_N, while in the optimal method this indicates the first N modes are used in Eq. (16). Obviously, the following relation holds for these three errors

$$e(N)\le e_t(N)+e_c(N)\,. \tag{28}$$

The truncation errors can be used to decide how many modes should be included in mode superposition. It is also used to determine the highest reference mode. The convergence error directly illustrates the validity of the reference frequencies in establishing the Caughey damping. Under harmonic ground motion described by Eq. (26) with $\theta_1=0.7\omega_9$, $\theta_2=1.25\omega_9$ and $\theta_3=2.8\omega_9$, the truncation errors are listed in Table 3. When N=24 and N=34, the relative errors $e(N)$ and the convergence errors $e_c(N)$ are presented in Table 5. For each Caughey damping coefficients, the average errors $\bar{e}$ and the coefficients of variation (COV) of peak responses are also listed in Tables 5.

As for Rayleigh damping (J=2) in the equipartition method, the errors are huge. It illustrates that arbitrarily specifying the two reference frequencies can cause unacceptable errors. It can also been observed that for both methods the convergence errors decrease when the term number of Caughey series increases. In terms of convergence speed, the optimal method is notably faster than the equipartition method. Moreover, negative damping is uncontrollable in the equipartition method, which will invalidate the results of analysis. The errors will approach zero when increasing the number of terms in the optimal method. The relative error is the total effect of the truncation error and convergence error. The truncation error is like a system error, while the relative errors will oscillate around the truncation error. Therefore, the optimal solution should include modes contributing significantly to all responses, and control the truncation error to an acceptable level.

Table 5a Errors (%) by the equipartition method for N=24

Response	$e_c(24)$			$e(24)$		
	J=2	J=4	J=6	J=2	J=4	J=6
u_{yA}	4.883	0.326	0.228	4.915	0.358	0.195
u_{yB}	81.842	5.908	0.869	81.842	5.908	0.869
F_N	31.142	1.233	0.228	29.543	2.831	1.370
$\bar{e}$	39.289	2.489	0.442	38.767	3.032	0.811
COV	0.996	1.204	0.838	1.013	0.917	0.726

Table 5b Errors (%) by the optimization method with $\phi_{kn}=\phi_n(\mathrm{A_y})$ for N=24

Response	$e_c(24)$				$e(24)$			
	J=2	J=4	J=6	J=8	J=2	J=4	J=6	J=8
u_{yA}	0.684	0.033	0	0	0.651	0	0.033	0.033
u_{yB}	0.695	0	0	0	0.695	0	0	0
F_N	1.233	1.370	0	0	2.831	0.228	1.598	1.598
$\bar{e}$	0.871	0.467	0	0	1.392	0.076	0.544	0.544
COV	0.361	1.672	0	0	0.895	1.732	1.680	1.680

Table 5c Errors (%) by the equipartition method for N=34

Response	e_c(34)			e(34)		
	J=2	J=4	J=6	J=2	J=4	J=6
u_{yA}	11.165	2.181	0.814	11.165	2.181	0.814
u_{yB}	174.196	35.882	2.954	174.196	35.882	2.954
F_N	68.128	12.283	1.735	67.671	11.826	1.279
$\overline{e}$	84.497	16.782	1.834	84.344	16.630	1.682
COV	0.979	1.031	0.585	0.982	1.044	0.669

Table 5d Errors (%) by the optimization method with $\phi_{kn} = \phi_n(A_y)$ for N=34

Response	e_c(34)				e(34)			
	J=2	J=4	J=6	J=8	J=2	J=4	J=6	J=8
u_{yA}	0.651	0	0	0	0.651	0	0	0
u_{yB}	0.695	0	0	0	0.695	0	0	0
F_N	2.374	0.411	0.046	0	2.831	0.046	0.411	0.457
$\overline{e}$	1.240	0.137	0.015	0	1.392	0.015	0.137	0.152
COV	0.792	1.732	1.732	0	0.895	1.732	1.732	1.732

4.5 Influences of reference DOF

As shown in Figure 4, the reference DOF will affect the optimal results. Table 6 lists further the errors $e(N)$ and $e_c(N)$ with $\phi_{kn} = \phi_n(B_y)$ and $\phi_{kn} = 1$ for N=34. The convergence error shows that the reference DOF affects significantly for J=2. For $J \geq 4$, the difference of convergence errors with different reference DOFs is tiny and can be neglected. A closer examination of Figure 3 indicates that the curves of damping ratios are different for different reference DOFs, but the modal damping ratios in the significant contribution modes are almost equal. The reason is that the total numbers of significant contribution modes are limited. The difference of damping ratios for the modes contributing insignificantly can be neglected. Accordingly, when the term-number of the series increases, the reference DOF has less effect on the optimal solution. For practical applications, no reference DOF is needed for $\phi_{kn} = 1$, therefore, it is an alternative choice when there is no special optimal DOF to be taken as the reference.

Table 6a Errors (%) by the optimization method with $\phi_{kn} = \phi_n(B_y)$ for N=34

Response	e_c(34)				e(34)			
	J=2	J=4	J=6	J=8	J=2	J=4	J=6	J=8
u_{yA}	0.684	0.065	0	0	0.684	0.065	0	0
u_{yB}	0.087	0	0	0	0.087	0	0	0
F_N	3.105	0.502	0.046	0	3.562	0.046	0.411	0.457
$\overline{e}$	1.292	0.189	0.015	0	1.444	0.037	0.137	0.152
COV	1.237	1.444	1.732	0	1.287	0.905	1.732	1.732

Table 6b Errors (%) by the optimization method with $\phi_{kn} = 1$ for N=34

Response	e_c(34)				e(34)			
	J=2	J=4	J=6	J=8	J=2	J=4	J=6	J=8
u_{yA}	0.456	0.065	0.033	0	0.456	0.065	0.033	0
u_{yB}	0.174	0	0	0	0.174	0	0	0
F_N	0.320	0.502	0.137	0	0.776	0.046	0.320	0.457
$\overline{e}$	0.316	0.189	0.057	0	0.469	0.037	0.117	0.152
COV	0.446	1.444	1.266	0	0.643	0.905	1.498	1.732

5. Applications to seismic responses analysis

5.1 Earthquake ground motions and derivative of deformation response spectrum

The frequency contents of earthquake ground motion depend largely on the site classes. Four acceleration records from various earthquakes as shown in Figure 5 are selected to investigate the performance of the proposed method in seismic response analysis. Table 7 summarizes various ground motions, occurrence dates, and earthquake designations. The Kobe, El Centro, Parkfield and Tianjin waves are typical waves of very dense soil, stiff soil, medium stiff soil and soft clay sites, respectively. Peak accelerations are scaled to 0.35m/s^2. The deformation spectra of various ground motions under 7 damping ratios (ζ = 0.005, 0.01, 0.02, 0.03, 0.05, 0.10, 0.20) are also presented in Figure 5.

The curves of deformation spectra are irregular, and therefore the spectrum derivative $S'_d(\zeta_n^*, \omega_n)$ is often evaluated numerically. Following Pan et al. [21], the spectrum derivative is obtained from the following statistical relation [28]:

$$S_d(\zeta, \omega_n) = g_n(\omega_n) + h_n(\omega_n) \ln 100\zeta \,. \tag{29}$$

The coefficients $g_n(\omega_n)$ and $h_n(\omega_n)$ can be determined from linear regression by seven spectral values $S_d(\zeta_m,\omega_n)$ (m=1,2,…,7). Then, the derivatives $S'_d(\zeta_n^*, \omega_n)$ can be approximated by:

$$S'_d(\zeta_n^*, \omega_n) = h_n(\omega_n) / \zeta_n^* \tag{30}$$

in which $h_n = \dfrac{\sum_{m=1}^{7}\left(\ln 100\zeta_m - \bar{\zeta}\right)\left(S_d(\zeta_m, \omega_n) - \bar{S}_{dn}\right)}{\sum_{m=1}^{7}\left(\ln 100\zeta_m - \bar{\zeta}\right)^2}$, $\bar{\zeta} = \left(\sum_{m=1}^{7} \ln 100\zeta_m\right)/7$ and $\bar{S}_{dn} = [\sum_{m=1}^{7} S_d(\zeta_m, \omega_n)]/7$.

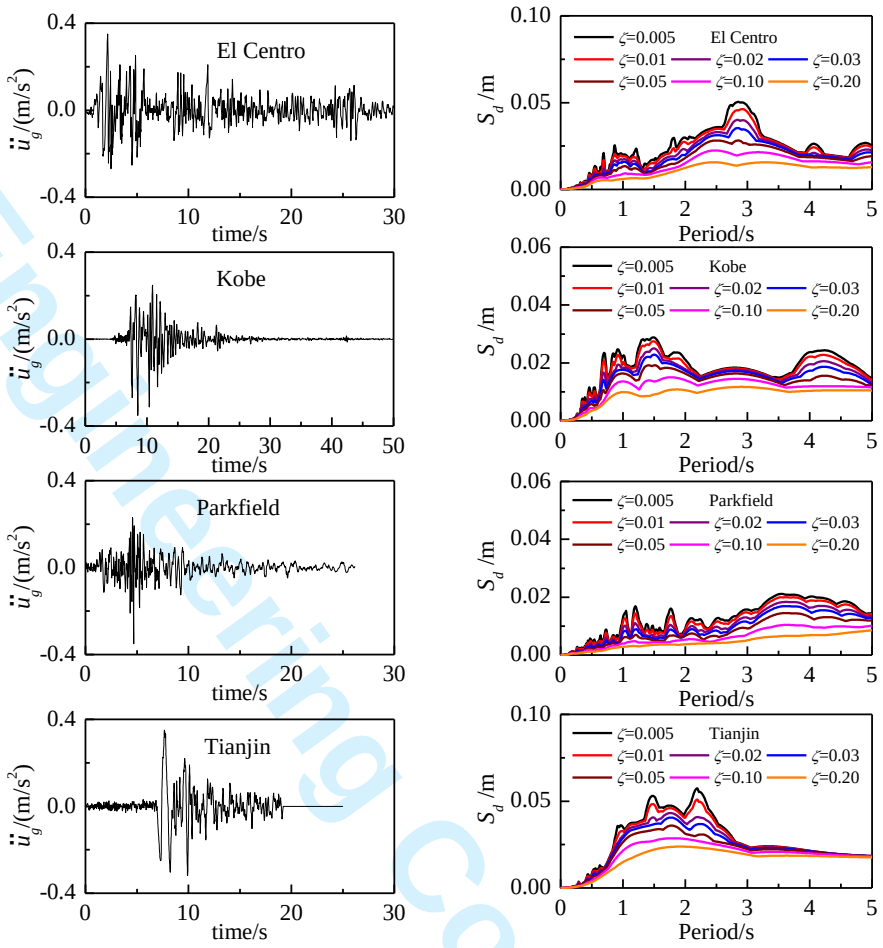

Figure 5 Acceleration time histories and its deformation response spectra

Table 7 Earthquake ground motions used in this study

Abbreviation	Ground Motion	Time	Earthquake
E1	El Centro	May 18, 1940	California earthquake
E2	Kobe	Jan. 17, 1995	Kobe earthquake
E3	Parkfield	Jun 27, 1966	Parkfield earthquake
E4	Tianjin	Nov 25, 1976	Tangshan aftershock

5.2 Vertical seismic response of a seven-story frame

The seven-story frame as shown in Figure 2 was considered. Under the four earthquake excitations, the truncation errors of u_{yA}, u_{yB} and F_N are summarized in Table 8, respectively. For the displacements u_{yA} and u_{yB}, the lower natural frequencies (mainly the 9th mode (6.166 Hz), 11th mode (6.473 Hz), 18th mode (7.420 Hz) and 20th mode (7.670Hz)) are the dominating modes, but higher modes until the 34th mode (39.306Hz) all contribute significantly to the foundation force. The first 34 modes are used to compute the optimal damping coefficients. Correspondingly, the 34th mode is taken as the highest mode in the equipartition method.

Under the four earthquake excitations, the convergence errors and relative errors of u_{yA}, u_{yB} and F_N are presented in Tables 9. Overall, Table 9 indicates that the proposed optimization method is significantly more accurate than the equipartition method in terms of average errors for both single response and three responses under all four earthquakes.

Table 8 Accumulated mode contributions and truncation errors of seven-story frame under earthquake excitations

Ground motion	Number of modes	u_{yA}		u_{yB}		F_N	
		Peaks(mm)	Error(%)	Peaks(mm)	Error(%)	Peaks(10^2kN)	Error(%)
E1	11	0.907	1.888	0.064	85.838	0.766	32.179
	20	0.894	0.472	0.453	0.310	0.941	16.696
	24	0.890	0.011	0.452	0	1.087	3.720
	34	0.890	0	0.452	0	1.118	0.974
	70	0.890	0	0.452	0	1.129	0
E2	11	0.679	5.597	0.045	77.180	0.537	38.583
	20	0.647	0.529	0.197	0.563	0.691	21.006
	24	0.643	0	0.195	0	0.825	5.691
	34	0.643	0.016	0.195	0	0.861	1.566
	70	0.643	0	0.195	0	0.875	0
E3	11	1.379	0.217	0.106	66.039	1.261	16.435
	20	1.382	0	0.314	0.319	1.441	4.506
	24	1.382	0	0.313	0.032	1.514	0.331
	34	1.382	0	0.313	0	1.506	0.199
	70	1.382	0	0.313	0	1.509	0
E4	11	0.518	4.966	0.037	83.036	0.437	47.583
	20	0.495	0.324	0.218	0.833	0.566	32.122
	24	0.493	0	0.216	0.046	0.763	8.480
	34	0.493	0	0.216	0	0.814	2.411
	70	0.493	0	0.216	0	0.834	0

Table 9a Errors (%) by the equipartition method subjected to earthquake excitations

Response	Ground motion	$e_c(34)$			$e(34)$		
		J=2	J=4	J=6	J=2	J=4	J=6
u_{yA}	E1	23.947	14.058	5.057	23.947	14.058	5.057
	E2	62.142	22.373	6.390	62.158	22.388	6.405
	E3	18.813	12.012	4.269	18.813	12.012	4.269
	E4	22.943	10.255	3.141	22.943	10.255	3.141
	$\bar{e}$	31.961	14.674	4.714	31.965	14.678	4.718
	COV	0.633	0.365	0.290	0.634	0.366	0.291
u_{yB}	E1	58.977	18.840	1.860	58.977	18.84	1.86
	E2	34.903	12.641	1.791	34.903	12.641	1.791
	E3	31.120	8.235	1.021	31.12	8.235	1.021
	E4	80.287	11.985	0.278	80.287	11.985	0.278
	$\bar{e}$	51.322	12.925	1.237	51.322	12.925	1.237
	COV	0.446	0.340	0.601	0.446	0.340	0.601
F_N	E1	22.586	11.160	4.429	21.612	10.186	3.454
	E2	28.309	11.874	3.257	26.743	10.309	1.691
	E3	2.717	2.651	1.458	2.518	2.452	1.259
	E4	3.514	2.579	1.511	1.104	0.168	0.900
	$\bar{e}$	14.282	7.066	2.664	12.994	5.779	1.826
	COV	0.918	0.729	0.542	1.008	0.907	0.620
$\bar{e}$		32.522	11.555	2.872	32.094	11.127	2.594
COV		0.722	0.489	0.647	0.743	0.545	0.725

Table 9b Errors (%) by the optimization method with $\phi_{kn} = \phi_n(A_y)$ subjected to earthquake excitations

Response	Ground motion	$e_c(34)$				$e(34)$			
		J=2	J=4	J=6	J=8	J=2	J=4	J=6	J=8
u_{yA}	E1	0.034	0.011	0	0	0.034	0.011	0	0
	E2	0	0	0	0	0.016	0.016	0.016	0.016
	E3	0	0	0	0	0	0	0	0
	E4	0	0.020	0	0	0	0.020	0	0
	$\bar{e}$	0.008	0.008	0	0	0.012	0.012	0.004	0.004
	COV	2.000	1.246	0	0	1.302	0.737	2.000	2.000
u_{yB}	E1	0.044	0.376	0	0	0.044	0.376	0	0
	E2	0.461	0.205	0	0	0.461	0.205	0	0
	E3	0.287	0.160	0.032	0	0.287	0.160	0.032	0
	E4	0.139	0	0.046	0	0.139	0	0.046	0
	$\bar{e}$	0.233	0.185	0.020	0	0.233	0.185	0.020	0
	COV	0.781	0.836	1.193	0	0.781	0.836	1.193	0
F_N	E1	1.949	0.620	0.266	0	2.923	0.354	0.709	0.974
	E2	1.520	1.200	0.240	0.011	0.046	0.366	1.326	1.577
	E3	0.199	1.193	0.133	0	0.398	0.994	0.066	0.199
	E4	1.859	1.415	0.432	0	0.552	0.996	1.979	2.411
	$\bar{e}$	1.382	1.107	0.268	0.003	0.980	0.677	1.020	1.290
	COV	0.586	0.308	0.463	2.000	1.340	0.541	0.805	0.726
$\bar{e}$		0.541	0.433	0.096	0.001	0.408	0.291	0.348	0.431
COV		1.411	1.246	1.496	3.464	1.999	1.237	1.886	1.857

Table 9c Errors (%) by the optimization method with $\phi_{kn} = \phi_n(B_y)$ subjected to earthquake excitations

Response	Ground motion	$e_c(34)$				$e(34)$			
		J=2	J=4	J=6	J=8	J=2	J=4	J=6	J=8
u_{yA}	E1	0.045	0.022	0.011	0	0.045	0.022	0.011	0
	E2	0.016	0.016	0	0	0.031	0.031	0.016	0.016
	E3	0	0	0	0	0	0	0	0
	E4	0	0.020	0	0	0	0.020	0	0
	$\bar{e}$	0.015	0.015	0.003	0	0.019	0.018	0.007	0.004
	COV	1.401	0.696	2.000	0	1.192	0.713	1.184	2
u_{yB}	E1	0.022	0	0	0	0.022	0	0	0
	E2	0	0	0	0	0	0	0	0
	E3	0	0	0	0	0	0	0	0
	E4	0.046	0	0	0	0.046	0	0	0
	$\bar{e}$	0.017	0	0	0	0.017	0	0	0
	COV	1.290	0	0	0	1.290	0	0	0
F_N	E1	1.949	0.797	0.266	0	2.923	0.177	0.709	0.974
	E2	1.566	1.303	0.309	0	0	0.263	1.257	1.566
	E3	0.199	0.994	0.133	0	0.398	0.795	0.066	0.199
	E4	1.859	2.147	0.612	0	0.552	0.264	1.799	2.411
	$\bar{e}$	1.393	1.310	0.330	0	0.968	0.375	0.958	1.287
	COV	0.583	0.454	0.614	0	1.367	0.756	0.775	0.726
$\bar{e}$		0.475	0.442	0.111	0	0.335	0.131	0.321	0.430
COV		1.684	1.614	1.743	0	2.494	1.779	1.895	1.857

Table9d Errors (%) by the optimization method with ϕ_{kn} = 1 subjected to earthquake excitations

Response	Ground motion	e_c(34)				e(34)			
		J=2	J=4	J=6	J=8	J=2	J=4	J=6	J=8
u_{yA}	E1	0.180	0.022	0.011	0	0.180	0.022	0.011	0
	E2	0.016	0	0	0	0.031	0.016	0.016	0.016
	E3	0.072	0	0	0	0.072	0	0	0
	E4	0	0.020	0	0	0	0.020	0	0
	$\bar{e}$	0.067	0.011	0.003	0	0.071	0.015	0.007	0.004
	COV	1.217	1.158	2.000	0	1.108	0.696	1.184	2.000
u_{yB}	E1	0.598	0.022	0	0	0.598	0.022	0	0
	E2	0.102	0.051	0	0	0.102	0.051	0	0
	E3	0.096	0	0	0	0.096	0	0	0
	E4	0	0	0	0	0	0	0	0
	$\bar{e}$	0.199	0.018	0	0	0.199	0.018	0	0
	COV	1.357	1.324	0	0	1.357	1.324	0	0
F_N	E1	1.683	0.886	0.354	0.089	2.657	0.089	0.620	1.063
	E2	1.566	1.451	0.251	0.023	0	0.114	1.314	1.589
	E3	0.133	0.464	0.133	0	0.331	0.265	0.066	0.199
	E4	1.859	2.519	0.672	0	0.552	0.108	1.739	2.411
	$\bar{e}$	1.310	1.330	0.352	0.028	0.885	0.144	0.935	1.315
	COV	0.606	0.669	0.656	1.504	1.359	0.566	0.792	0.706
$\bar{e}$		0.525	0.453	0.118	0.009	0.385	0.059	0.314	0.440
COV		1.390	1.760	1.781	2.780	1.936	1.308	1.911	1.838

Figure 6 and Figure 7 show damping ratios by various methods. The curves of damping raitos obtained by the optimal method vary with the earthquake excitations since the frequency contents of different seismic waves change. The damping ratio curve obtained by the equipartition method is independent of the excitations, and the errors fluctuate strongly for the same response under different excitations. For example, the e_c(34) of F_N are 11.874% and 2.651% for J=4 under Kobe and Parkfield ground motions respectively. This shows that the equipartition method can easily lead to significantly inconsistent results among various analysts in engineering practices. The exact modal damping ratios are the natural characteristics and independent of the load. But Caughey damping is an approximate damping matrix. It is necessary to choose the load-dependent reference frequencies to minimize the errors of modal damping ratios of significant contribution mode. Therefore, the errors by the optimization method always yield a lower average and COV. When J=8, the three types of reference DOFs all converge to the response with exact damping ratios for the first 34 modes. For J=6, the errors of all three responses are always less than 1%. A closer examination in Table 2 indicates that there are only seven significant contribution modes. The convergence errors are tiny for the optimal method due to the fact that all damping ratios for the seven significant modes are equal to the exact values for J=8, and six damping ratios of the seven significant modes are exact for J=6.

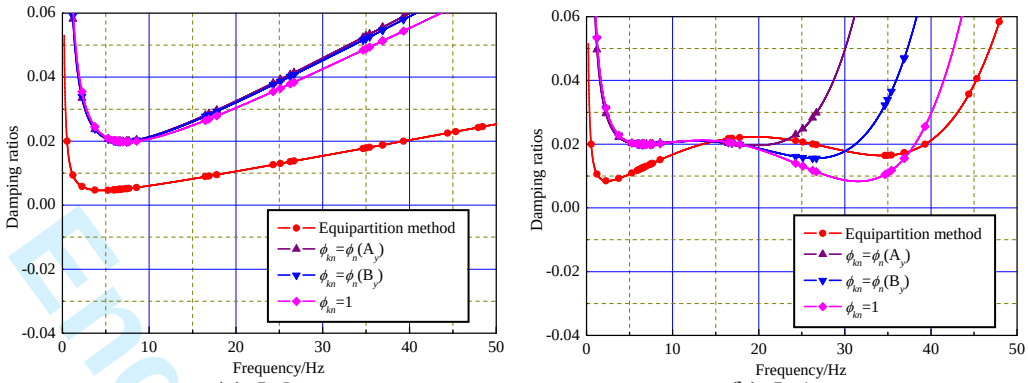

(a) J=2 (b) J=4

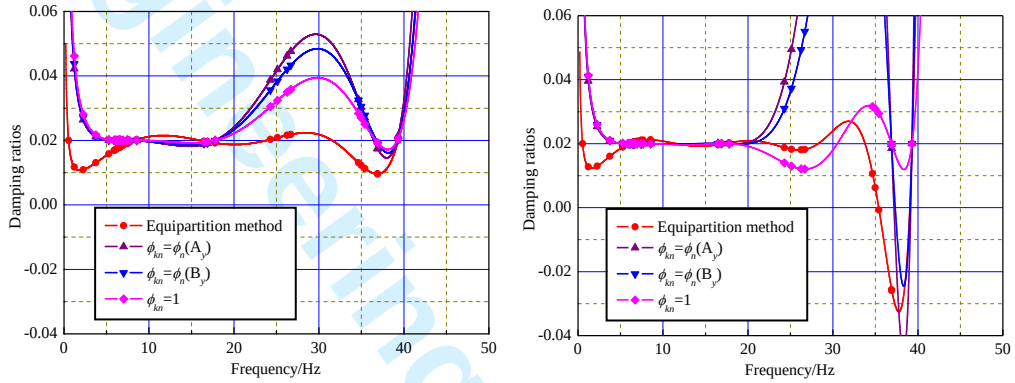

(c) J=6 (d) J=8

Figure 6 The influences of reference DOF on the damping ratios under El Centro Earthquake

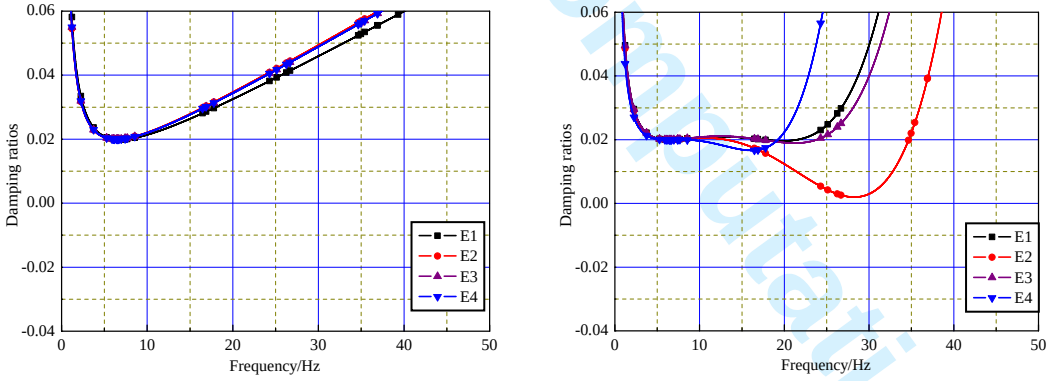

(a) J=2 (b) J=4

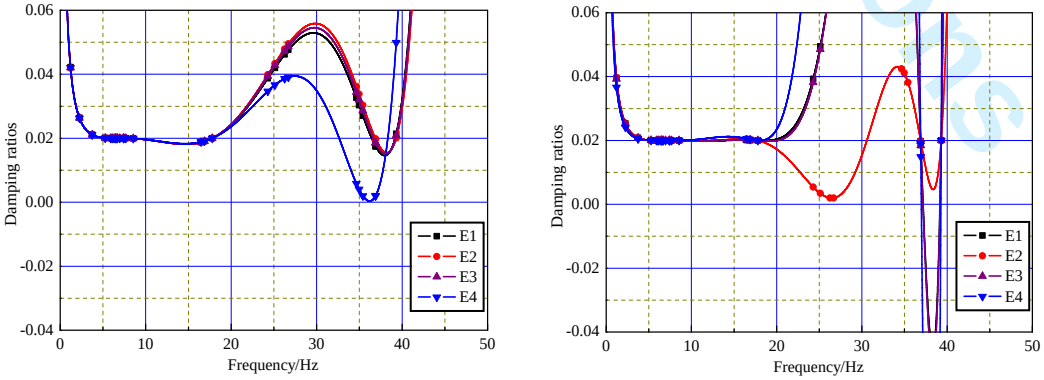

(c) J=6 (d) J=8

Figure 7 The influences of excitations on the optimal damping ratios for $\phi_{kn} = \phi_n(A_y)$

5.3 Horizontal seismic response of a shear building

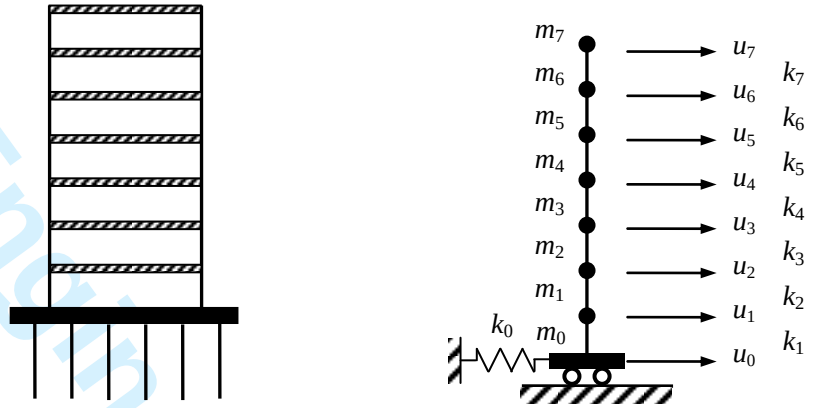

Figure 8 A seven-story shear building on massive stiffness foundation

A seven-story shear building is built on a massive foundation supported on stiff piles as shown in Figure 8a and its idealized computer model [22] is shown in Figure 8b. The parameters of the structure are listed in Table 10. Only eight modes can be used because the model has only eight masses. The natural frequency, mass participation factor and accumulated mass participation factor are shown in Table 11. It is apparent that the 8th mode is associated with the vibration of foundation mass and the natural frequency is far higher than the 7th natural frequency. The exact damping ratios are 5% for all modes of vibration. Peaks of the top displacement u_7, the first story displacement u_1 and the foundation force F_0 using different numbers of modes are summarized in Table 12. The corresponding truncation errors are also listed in Table 12.

Table 10 Model Parameters of seven-story shear building

m	m_0	m_1	m_2	m_3	m_4	m_5	m_6	m_7
(×100kg)	26	8	6	2	6	2	1	1
k	k_0	k_1	k_2	k_3	k_4	k_5	k_6	k_7
(×20kN/m)	2760	12	8	4	4	2	1	1

Table 11 Results of modal analysis of the frame

Mode	Frequency (Hz)	Lateral mass participating factor	
		Each (%)	Accumulated (%)
1	0.719	30.767	30.767
2	1.404	6.452	37.218
3	2.165	10.348	47.566
4	2.848	0.478	48.044
5	3.835	0.115	48.159
6	4.000	2.221	50.38
7	4.989	0.061	50.441
8	23.241	49.559	100

Table 12 Accumulated mode contributions and truncation errors of seven-story shear building

under earthquake excitations

Ground motion	Number of modes	u_7		u_1		F_0	
		Peaks(mm)	Error(%)	Peaks(mm)	Error(%)	Peaks(kN)	Error(%)
E1	2	21.83	2.392	1.545	26.985	0.370	67.835
	3	21.41	0.422	2.160	2.079	0.519	54.843
	6	21.32	0	2.121	0.236	0.510	55.670
	7	21.32	0	2.116	0	0.509	55.757
	8	21.32	0	2.116	0	1.150	0
E2	2	37.59	6.699	3.069	27.24	0.735	46.129
	3	35.63	1.135	4.298	1.897	1.031	24.413
	6	35.23	0	4.221	0.071	1.012	25.806
	7	35.23	0	4.218	0	1.012	25.806
	8	35.23	0	4.218	0	1.364	0
E3	2	10.25	0.582	0.922	17.513	0.221	73.540
	3	10.25	0.582	1.108	0.894	0.267	68.013
	6	10.31	0	1.119	0.089	0.270	67.69
	7	10.31	0	1.118	0	0.269	67.714
	8	10.31	0	1.118	0	0.834	0
E4	2	65.06	0.046	4.421	16.11	1.058	33.165
	3	65.05	0.031	5.107	3.093	1.223	22.742
	6	65.03	0	5.270	0	1.263	20.215
	7	65.03	0	5.270	0	1.263	20.215
	8	65.03	0	5.270	0	1.583	0

For the case of u_7 and u_1, using only the first three modes is enough to estimate these responses. But the accumulated mass participation factor of the first 7 modes is only 50.441%. It will cause a significant error for the estimation of the foundation force if only the first 7 modes were used. Therefore, all modes are used in the optimization method and the equipartition method.

Under the four earthquake excitations, the relative errors of u_7, u_1 and F_0 are presented in Table 13. Once again, the proposed optimization method is significantly more accurate than the equipartition method for ϕ_{kn}=1. But the results of foundation force for J=4 and J=6 with $\phi_{kn}=\phi_n(u_7)$ as well as J=4 with $\phi_{kn}=\phi_n(u_1)$ are less favorable to the proposed method for the determination of Caughey damping coefficients. To investigate the reason of significant errors in these cases, the normalized weighted coefficients are listed in Table 14. Associated curves of damping ratios are shown in Figure 9 and Figure 10. If u_7 is used as the reference DOF, the normalized weighted coefficient associated with the 8th mode is far less than other modes. The main reason is that the normalized mode displacement of u_7 is trivial in the 8th mode just like a node of mode. Therefore, the effect of the 8th mode is neglected in the optimal solution. It indicates that the reference DOF should bypass nodes of modes. Setting ϕ_{kn}=1 will eliminate this problem, achieving excellent results even under extreme conditions.

When J=8, the desired damping ratio is obtained exactly at the eight specified frequencies. Therefore, the Caughey damping coefficients solved in Eq. (16) are independent of the reference DOF and ground motions.

Table 13a Relative errors (%) subjected to earthquake excitations

Response	Ground motion	Equipartition method				Optimal method with ϕ_{kn}=1			
		J=2	J=4	J=6	J=8	J=2	J=4	J=6	J=8
u_7	E1	8.161	5.675	4.128	3.049	1.970	1.079	0	0
	E2	3.775	1.079	1.135	1.022	0.908	0.397	0	0
	E3	3.783	2.619	1.843	1.261	0.097	0	0	0
	E4	1.184	0.846	0.600	0.431	0.138	0.062	0	0

	$\bar{e}$	4.226	2.555	1.926	1.441	0.778	0.384	0	0
	COV	0.685	0.871	0.806	0.783	1.127	1.287	0	0
u_1	E1	53.403	33.885	20.747	12.476	1.938	1.087	0.047	0
	E2	33.239	20.081	12.162	7.421	1.778	0.569	0.119	0
	E3	38.819	23.256	12.791	7.871	3.399	1.252	0.179	0
	E4	7.799	5.237	3.435	2.201	0.171	0.171	0.019	0
	$\bar{e}$	33.315	20.615	12.284	7.492	1.821	0.770	0.091	0
	COV	0.571	0.574	0.576	0.561	0.725	0.642	0.793	0
F_0	E1	3.217	1.826	1.043	0.522	2.087	0.174	0	0
	E2	11.657	5.572	2.493	0.806	0.220	2.126	0.073	0
	E3	6.642	2.877	1.115	0.348	4.340	5.371	0.036	0
	E4	6.317	4.169	2.653	1.706	0.569	0.379	0	0
	$\bar{e}$	6.958	3.611	1.826	0.845	1.804	2.013	0.027	0
	COV	0.502	0.449	0.474	0.714	1.039	1.195	1.282	0
$\bar{e}$		14.833	8.927	5.345	3.259	1.468	1.056	0.039	0
COV		1.152	1.201	1.195	1.192	0.940	1.417	1.465	0

Table13b Relative errors (%) subjected to earthquake excitations

Response	Ground motion	Optimal method with $\phi_{kn} = \phi_n(u_7)$				Optimal method with $\phi_{kn} = \phi_n(u_1)$			
		J=2	J=4	J=6	J=8	J=2	J=4	J=6	J=8
u_7	E1	1.313	0	0	0	1.923	1.407	0	0
	E2	0.852	0	0	0	0.397	0	0.028	0
	E3	0.388	0	0	0	0.097	0.097	0	0
	E4	0.015	0.015	0	0	0.231	0.108	0	0
	$\bar{e}$	0.642	0.004	0	0	0.662	0.403	0.007	0
	COV	0.877	2.000	0	0	1.283	1.666	2.000	0
u_1	E1	3.214	0.425	0.142	0	3.828	0.898	0.047	0
	E2	4.433	0.735	0.024	0	0.403	0.545	0	0
	E3	7.245	0.626	0.089	0	1.073	0.447	0.089	0
	E4	1.271	0.038	0.019	0	0.683	0.247	0	0
	$\bar{e}$	4.041	0.456	0.068	0	1.497	0.534	0.034	0
	COV	0.619	0.673	0.854	0	1.054	0.510	1.260	0
F_0	E1	2.783	55.461	55.704	0	1.652	2.000	0	0
	E2	0.880	26.173	25.806	0	0.293	24.487	0	0
	E3	5.923	68.013	67.690	0	2.362	67.774	0.060	0
	E4	1.579	19.962	20.152	0	0.190	18.320	0	0
	$\bar{e}$	2.791	42.402	42.338	0	1.124	28.145	0.015	0
	COV	0.799	0.544	0.543	0	0.943	0.997	2.000	0
$\bar{e}$		2.491	14.287	14.136	0	1.094	9.694	0.019	0
COV		0.924	1.680	1.701	0	1.046	2.065	1.641	0

Table 14 Normalized weighted coefficients

ϕ_{kn}	Ground motion	Mode							
		1	2	3	4	5	6	7	8
$\phi_n(u_7)$	E1	7.44E-1	1.97E-1	5.78E-2	4.81E-4	9.76E-5	3.75E-5	8.54E-10	2.47E-32
	E2	7.39E-1	2.47E-1	1.28E-2	9.21E-4	1.74E-5	7.99E-7	1.35E-11	3.06E-35
	E3	7.27E-1	2.62E-1	9.90E-3	2.65E-4	2.48E-4	8.65E-6	9.72E-10	3.85E-35
	E4	9.88E-1	1.11E-2	8.11E-4	2.30E-5	2.79E-6	7.53E-7	3.37E-11	4.17E-36
$\phi_n(u_1)$	E1	1.11E-1	4.38E-2	8.25E-1	3.16E-4	4.93E-5	1.97E-2	1.09E-5	2.03E-9
	E2	3.16E-1	1.57E-1	5.24E-1	1.73E-3	2.51E-5	1.20E-3	4.92E-7	7.18E-12

	E3	3.47E-1	1.86E-1	4.51E-1	5.56E-4	4.00E-4	1.45E-2	3.95E-5	1.01E-11
	E4	9.11E-1	1.52E-2	7.14E-2	9.30E-5	8.67E-6	2.43E-3	2.64E-6	2.11E-12
1	E1	7.11E-1	9.24E-2	1.94E-1	5.44E-4	1.10E-4	1.93E-3	1.65E-5	1.89E-6
	E2	8.15E-1	1.34E-1	4.98E-2	1.20E-3	2.26E-5	4.74E-5	3.03E-7	2.71E-9
	E3	8.15E-1	1.44E-1	3.91E-2	3.52E-4	3.27E-4	5.22E-4	2.21E-5	3.46E-9
	E4	9.92E-1	5.46E-3	2.86E-3	2.73E-5	3.29E-6	4.06E-5	6.86E-7	3.36E-10

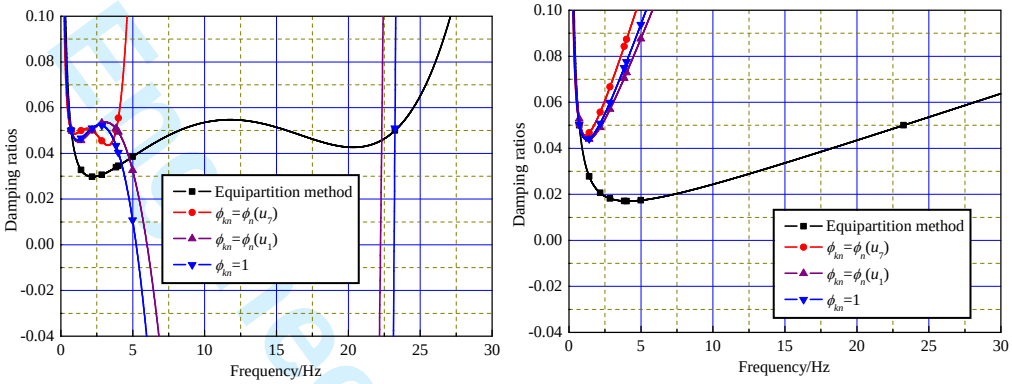

(a) J=2 (b) J=4

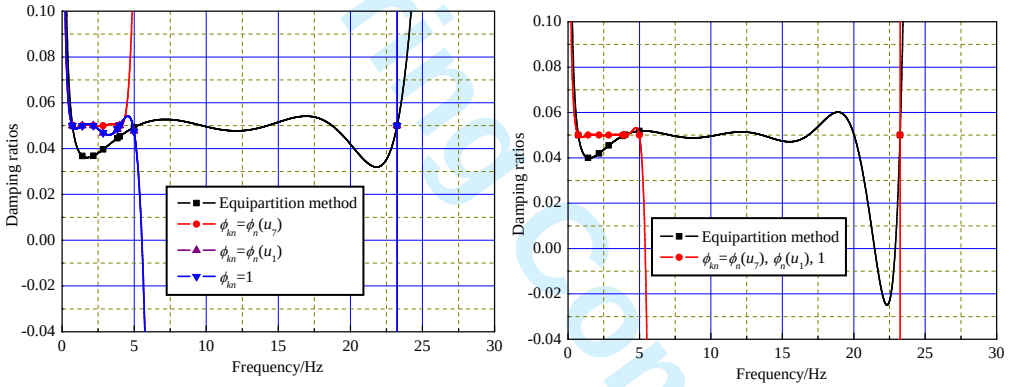

(c) J=6 (d) J=8

Figure 9 The influences of reference DOF on the damping ratios under El Centro earthquake

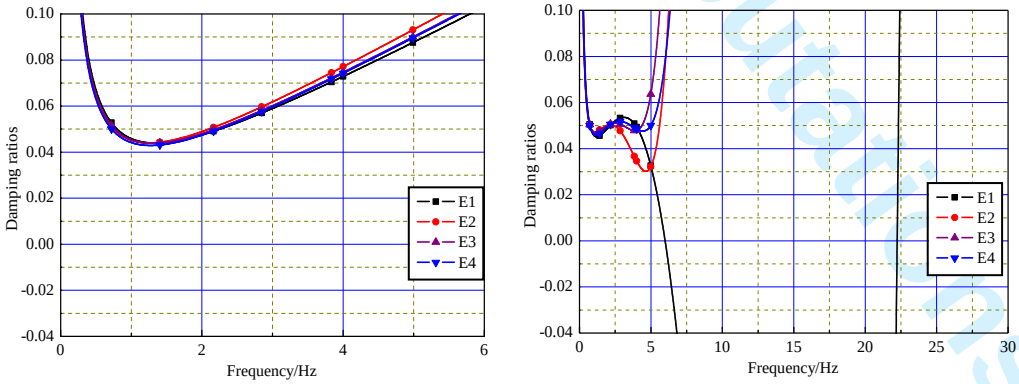

(a) J=2 (b) J=4

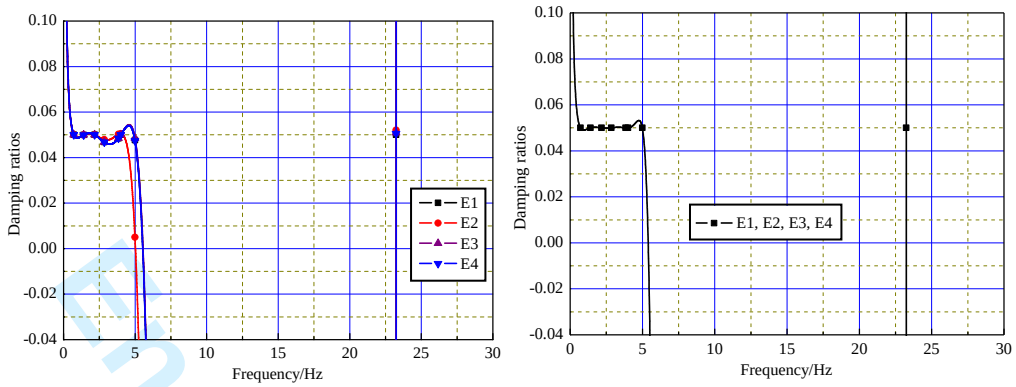

(c) J=6 (d) J=8

Figure 10 The influences of excitations on the optimal damping ratios for $\phi_{kn} = \phi_n(u_1)$

6. Conclusion

Caughey damping is suitable when damping ratios of more than two modes are desired to be equal to recommended/measured values. In this paper, a constrained optimization method is proposed for evaluation of Caughey damping coefficients. The objective function can be defined as any error term of peak structural displacements of engineering interests subject to that all modal damping ratios are positive. Based on extensive analyses and numerical results, the following conclusions can be drawn:

(1) The main advantage of the proposed method is that the Caughey damping coefficients are automatically determined which eliminates the arbitrariness in current experience-based practices. Moreover, the optimal Caughey coefficients can ensure reasonable damping ratios for all modes contributing significantly to the response. As a comparison, it is noted that the widely used equipartition method can cause inconsistent accuracies when a structure is subject to different excitations and suffer the risk of negative damping due to Runge's phenomenon.

(2) To choose the exponent combination of Caughey series, the extended Rayleigh exponents approach is recommended, while the symmetrical exponent combination can cause impractical negative damping.

(3) The choice of the reference DOF is important for the lower order Caughey series. Because the limited significant contribution modes, the effects of the reference DOF on errors will decrease with the increase of term number. Therefore, using ϕ_{kn} =1 is a simplified method for practical applications.

(4) The proposed optimization method can be viewed as a generalization of the conventional Caughey method. For more than 4 order Caughey series, the dynamic response will cause truncation errors due to the Runge phenomenon. By including all important modes of vibration in the objective function, the results will converge to the exact cumulative mode response when the term-number increases.

(5) The exact modal damping ratios are the natural characteristics and independent of the load. But Caughey damping is an approximate damping matrix. It is necessary to choose the load-dependent reference frequencies to minimize the errors of modal damping ratios of significant contribution modes. Thus, the damping matrix should be recomputed each time when the loading condition changes. Compared to the conventional method and the equipartition method, the Caughey damping coefficients obtained by the proposed method includes the effects of both the dynamic characteristics of the structure and frequency content of excitations. The new method improves the accuracy significantly while being convenient to apply in engineering practice.

Acknowledgements

The research work was supported by the Open Foundation of State Key Laboratory for Disaster Reduction in Civil Engineering (SLDRCE15-01). The authors would also like to thank European Community's Seventh Framework Programme (Marie Curie International Research Staff Exchange Scheme, Grant No. 612607) and the Sêr Cymru National Research Network in Advanced Engineering and Materials.

References

[1] FEMA356. Prestandard and commentary for seismic rehabilitation of buildings [S]. Prepared by American Society of Civil Engineers for the Federal Emergency Management Agency, Washington DC, 2000.

[2] Chopra AK. Dynamics of Structures: Theory and Applications to Earthquake Engineering [M]. New Jersey: Englewood Cliffs, Prentice-Hall, 1995.

[3] Clough R, Penzien J. Dynamics of Structures (Third edition) [M]. Computers and structures Inc, 2003.

[4] Wilson EL, Penzien J. Evaluation of orthogonal damping matrices [J]. International Journal for Numerical Methods in Engineering, 1972, 4: 5–10.

[5] Adhikari S. Damping Modeling Using Generalized Proportional Damping [J]. Journal of sound and vibration, 2006, 293(1-2): 156-170.

[6] Prishati R. Seismic response of low-rise steel moment-resisting frame (SMRF) buildings incorporating nonlinear soil–structure interaction (SSI) [J]. Engineering Structures, 2011, 33:958-967.

[7] Chiara C, Rui P. Seismic response of continuous span bridges through fiber-based finite element analysis [J]. Earthquake Engineering and Engineering Vibration, 2006, 5(1): 119-131.

[8] Khan E, Sullivan T J, Kowalsky M J. Direct displacement-based seismic design of reinforced concrete arch bridges[J]. Journal of Bridge Engineering, 2013, 19(1): 44-58.

[9] Zhang CH, Pan JW, Wang JT. Influence of seismic input mechanisms and radiation damping on arch dam response [J]. Soil Dynamic and Earthquake Engineering, 2009, 29: 1282-1293.

[10] Chen ZH, Qiao Wt, Wang XD. Seismic response analysis of long-span suspen-dome under multi-support excitations [J]. Transactions of Tianjin University, 2010, 16(6): 424-432.

[11] Xu J. A synthesis formulation of explicit damping matrix for non-classically damped systems [J]. Nuclear Engineering and Design, 2004, 227 (2): 125-132.

[12] Bilbao A, Aviles R, Agirrebeitia J and Ajuria D. Proportional damping approximation for structures with added viscoelastic dampers [J]. Finite Elements in Analysis and Design, 2006, 42 (6): 492-502.

[13] Mánica M, Ovando E, Botero E. Assessment of damping models in FLAC [J]. Computers and Geotechnics, 2014, 59: 12-20.

[14] Hall JF. Problems encountered from the use (or misuse) of Rayleigh damping [J]. Earthquake Engineering and Structural Dynamics, 2006, 35: 525 –545.

[15] Ryan KL, Polanco J. Problems with Rayleigh damping in base-isolated buildings [J]. Journal of Structural Engineering, ASCE, 2008, 134(11):1780 – 1784.

[16] Zareian F, Medina RA. A practical method for proper modeling of structural damping in inelastic plane structural systems [J]. Computers and structures, 2010, 88, 45-53.

[17] Jehel P, Léger P, Ibrahimbegovic A. Initial versus tangent stiffness-based Rayleigh damping in inelastic time history seismic analysis [J]. Earthquake Engineering and Structural Dynamics, 2014, 43(3):467-484.

[18] Pant DR, Wijeyewickrema AC, Elgawady MA. Appropriate viscous damping for nonlinear time-history analysis of base-isolated reinforced concrete buildings [J]. Earthquake Engineering and Structural Dynamics, 2013, 42: 2321-2339.
[19] Tsai CC, Park D, Chen CW. Selection of the optimal frequencies of viscous damping formulation in nonlinear time-domain site response analysis [J]. Soil Dynamics and Earthquake Engineering, 2014, 67: 353-358.
[20] Yang DB, Zhang YG, Wu JZ. Computation of Rayleigh Damping Coefficients in Seismic Time- History Analysis of Spatial Structures [J]. Journal of the International Association for Shell and Spatial Structures, 2010, 51(2): 125-135.
[21] Pan Danguang, Chen Genda, Wang Zuocai. Optimal Rayleigh damping coefficients in seismic analysis of viscously-damped structures [J]. Earthquake engineering and engineering vibration, 2014, 13(4):653-670.
[22] Wilson E L. Three-dimensional static and dynamic analysis of structures (Third edition) [M]. California: Computers and structures Inc, 2002.
[23] Dong Jun, Deng Hongzhou, Wang Zhaomin. Studies on the Damping Models for Structural Dynamic Time History Analysis [J]. World Information on Earthquake Engineering, 2000, 16(4): 63-69. (in Chinese)
[24] Caughey T K, O'Kelly M E J. Classical normal modes in damped linear dynamic systems [J]. Transactions of ASME, Journal of Applied Mechanics, 1965, 32: 583–588.
[25] Luco JE. A Note on Classical Damping Matrices [J]. Earthquake Engineering and Structural Dynamics, 2008, 37(4): 615-626.
[26] Andreas Antoniou, Wu-Sheng Lu. Practical optimization algorithms and engineering applications [M]. Spinger, 2007.
[27] Walter Gautschi. Numerical analysis: an introduction [M]. Birkhauser Boston, 1997.
[28] Newmark N M, Hall W J. Earthquake spectra and design, Earthquake engineering research institute [R]. California: Berkeley, 1982, 29-37.